Fermi National Accelerator Laboratory

FERMILAB-Conf-91/288-E

QCD Results from CDF

The CDF Collaboration

presented by R. Plunkett

Fermi National Accelerator Laboratory
P.O. Box 500, Batavia, Illinois 60510

October 1991

* Presented at the *Joint International Lepton-Photon Symposium and Europhysics Conference on High Energy Physics*, Geneva, Switzerland, July 25 - August 1, 1991.

CDF/PUB/JET/PUBLIC/1596
FERMILAB-CONF-91/288-E

QCD RESULTS FROM CDF

The CDF Collaboration
Presented by Robert Plunkett
Fermi National Accelerator Laboratory
Batavia, IL 60510, USA

ABSTRACT

Results are presented for hadronic jet and direct photon production at $\sqrt{s}$ = 1800 GeV. The data are compared with next-to-leading QCD calculations. A new limit on the scale of possible composite structure of the quarks is also reported.

High energy $\bar{p}p$ collisions produce a large rate of hadronic jets by the mechanism of hard partonic scattering. This scattering is generally described by the theory of Quantum Chromodynamics (QCD), either via leading-log shower Monte Carlo techniques [1], or by explicit perturbative calculations. Recently, several groups have published computations of jet production to next-to-leading order in the strong coupling constant α_s (order $\alpha_s{}^3$) [2,3]. These calculations and others will reduce the theoretical error associated with perturbative QCD calculations; it has been suggested [4] that a characteristic precision of 20% may soon be typical of the field. In addition, new dynamical distributions involving partonic radiation are now calculable and available for experimental testing.

The Tevatron collider provides an ideal laboratory for these tests, since the jet production spectrum extends over many orders of magnitude in the jet transverse energy E_t . In this paper we describe recent measurements of jet and direct photon production at the CDF experiment at the Tevatron, and compare those results with recent predictions of perturbative QCD.

Jets at CDF are identified as localized deposits of calorimetric energy, identified by a cone algorithm paramtetrized by a cone radius $R = \sqrt{(\Delta\eta^2) + (\Delta\phi^2)}$, where η is the pseudo-rapidity, and ϕ is the azimuthal angle w.r.t the line defined by the colliding beams. Cone radii used in this paper range from $R = 0.4$ to $R = 1.0$. The transverse energy E_t is defined as $E sin\theta$, where θ is the angle between the beamline and a line from the event vertex to the center of the jet cluster. The algorithm is fully described in [5]. The central calorimeter, used in the measurements described here, consists of projective towers of metal absorber-scintillator sandwich construction. They cover an η-range of $|\eta| < 1.1$, and the full range in ϕ. The calorimeter encloses the central tracking chamber (CTC), which measures track momenta in a 1.4 T solenoidal magnetic field.

The observed jet response in the calorimeter differs from the true E_t due to the effects of detector cracks and nonlinearity. We determine the magnitude of these effects using a combination of testbeam data and isolated tracks in the CTC to measure the calorimeter response to single pions to a precision of approximately 5%. This response, combined with fragmentation information from tracks in jets, can be used to simulate observed jets and obtain the required corrections. The procedure may be used to correct the average E_t of jets or additionally to incorporate the effects of resolution, which modifies the shape of any steeply falling E_t spectrum.

We have measured the inclusive E_t spectrum of jets using a trigger which required a single high-E_t calorimeter cluster above thresholds which ranged from 20 GeV to 60 GeV (the lower Et thresholds were prescaled). This trigger was determined to be > 98% efficient for jets with measured E_t between 35-100 GeV, depending on threshold. We imposed this cut on the jets, and also required an event vertex within 60 cm of the nominal beam interaction point, and that the jets fall in the range $0.1 < |\eta| < 0.7$. These cuts guarantee uniform energy measurement in the central calorimeter. We rejected cosmic ray background as in [6].

Published Proceedings Joint International Lepton-Photon Symposium and Europhysics Conference on High Energy Physics, Geneva, Switzerland, July 25-August 1, 1991.

Figure 1 shows the inclusive jet cross-section for a clustering radius $R = 0.7$, along with a prediction of next-to-leading order QCD using HMRSB structure functions [7] and a renormalization scale of $\mu = E_t$. The data have been corrected for energy losses and resolution smearing as discussed above. The corrections include the effect of contributions to the jet energy from the underlying event not associated with the hard scattering process. We make no correction for energy falling outside the clustering cone, as this should be accounted for in next-to-leading order calculations. The data and the calculation show good agreement over 7 orders of magnitude of cross-section.

Figure 2 contains the same data plotted as the fractional difference of the data with the HMRSB calculation ($\mu = E_t$). The dotted lines represent the E_t -independent part of the systematic error. The data points include statistical and E_t -dependent systematic error. The systematic error is typically 25%. A number of other theoretical predictions are also displayed to exhibit the variation with structure functions. Fits of theoretical curves to the data (for E_t >80 GeV) yield normalizations between 1.15 (HMRSB) to 1.29 (MTB1). HMRSE structure functions result in a poor fit to the data. The expected theoretical error (estimated from μ variation) is estimated at approximately 10% for this cone size.

Perturbative calculations at order $\alpha_s^{\ 3}$ predict that the measured inclusive jet cross-section will depend on the choice of cluster cone radius R. We measured the cross-section at three choices of cone radius, 0.4, 0.7, and 1.0. Threshold choices and corrections were done independently for each cone size. The results were fit to a function of the form $A + B \ln R$, yielding best fits of $A = 0.79 \pm 0.02$ nb/GeV and $B = 0.49 \pm 0.03$ nb/GeV, for jets of 100 GeV E_t . (For more details on next-to-leading order computations, see the contributions of S. Ellis and P. Chiapetta, these proceedings.)

Our data may be used to search for the presence of quark substructure, which can manifest itself as an enhancement in the cross-section at high jet E_t . This effect is conventionally written as a 4-Fermi interaction characterized by a constant Λ_C, with units of energy. Currently, only leading order calculations that include this contact term are available. We therefore fit the spectrum to leading-order QCD in the region 80GeV $< E_t <$160 GeV, where effects of $\Lambda_C > 750$ GeV are negligible. An overall normalization factor is the only free parameter in the fit. We use a cone size of 1.0 to minimize effects of energy loss out of the cone, not accounted for at this order in the theory.

We extrapolate the fitted curves to the region $E_t <$160 GeV for various values of Λ_C, and compare with the data. Point-to-point correlations are included for the E_t -dependent systematic error. We find the limit using the structure function sets HMRSB,MTS, and MTB [7,8]. The set HMRSE yielded poor fits in the region below 160 GeV, and was excluded. In this way we derive a limit on Λ_C of 1400 GeV, at the 95% confidence level.

Next-to-leading order QCD calculations provide, for the first time in a perturbative calculation, information on the internal distribution of energy within a jet. We have measured the internal p_t flow inside jets using tracking information from the CTC. The jets are selected by requiring them to be central ($0.1 < |\eta| < 0.7$), to have an event vertex within 60 cm of the interaction point, and to have E_t in the range 95 GeV $< E_t <$ 120 GeV (corrected). This selects about 18% of the triggers which required a 60 GeV trigger cluster. We use a cluster cone radius of $R = 1.0$.

Tracks pointing inside the cone radius are selected if they pass cuts on the occupancy (50% of the expected hits present) and have sufficient 3-dimensional reconstruction. For each selected track, we compute the distance r, in η-ϕ space, measured to the jet calorimeter centroid. We make the p_t density distribution

$$\rho(r) = \frac{1}{N} \sum_{jets} \frac{1}{P_t(1.0)} \frac{dp_t}{dr}$$

where $P_t(1.0)$ is the total transverse momentum carried by tracks inside the cluster cone, and N is the total number of jets in the sample.

Figure 3 shows the integral of $\rho(r)$ compared to an $\alpha_s^{\ 3}$ computation [9] using HMRSB structure functions and $\mu = E_t$. The distribution is normalized to P_t (1.0) as defined above. The

data have been corrected for tracking efficiency. We estimate this efficiency as functions of jet E_t and spacial separation of the tracks by injecting Monte Carlo tracks into real jet events. The theoretical calculation is expected, at this order, to vary somewhat with choice of renormalization scale μ.

The dominant systematic error for the integral distribution comes from the accuracy with which the jet axis can be determined. This has a its largest effect close to the jet core, (where the distribution is steeper), where it causes an uncertainty of 25%. Other effects are the uncertainty in the tracking correction, taken as its full value of 7% in the jet core, and the effects of jet E_t resolution, which causes a 6% effect in the core. The systematic uncertainty is greatly reduced as one moves away from the jet core, falling to about 4% at $R = 0.4$.

Jets in the central calorimeter can also be used to compute the dijet invariant mass and to measure its spectrum. We define the mass as $M_{jj} = \sqrt{(E_1 + E_2)^2 + (p_1 + p_2)^2}$, where p is the vector momentum, measured in the calorimeter. The two most energetic jets in the event are used to compute the mass. We require both jets to satisfy requirements on η ($|\eta| < 0.7$) and to have an event vertex near the interaction point. The trigger was as discussed for the inclusive jet cross-section measurement. This analysis required measured dijet mass thresholds of 120-280 GeV for a cone of 1.0 and 100-240 GeV for a cone of 0.7. Jets in the region $|\eta| < 0.1$ encounter a region of partial coverage in the CDF detector. For this reason we apply an η-dependent correction to the E_t of jets used in this measurement. The correction map is derived from a study of the p_t balance of dijet events, where one jet is well-measured.

The data can be compared to a leading order QCD computation. In doing this we apply no corrections for underlying event energy or energy falling out of the clustering cone, nor do we apply a cut in the $\Delta\phi$ of the two leading jets. We instead treat these effects as phenomenological uncertainties when fitting the data to theoretical predictions.

We have compared the data to leading-order QCD for two values of the cluster cone radius, $R = 0.7$ and $R = 1.0$. We convolve the theoretical curve with the jet resolution and response, rather than correcting the observed energies as in the inclusive jet cross-section. The correlations in the systematic errors are included in our fits. The systematic errors are dominated by calorimetry and fragmentation modeling, and are typically 50-55% of the value of the cross-section. Our fits to QCD allow a global normalization factor as a free parameter. Fits were performed for many choices of structure functions (DO, EHLQ, HMRS, and MT sets), and for several values of renormalization scale. We find in every case much improved statistical agreement using a cone size of 1.0. The confidence level for $R = 0.7$ is never greater than 10%, while the $R = 1.0$ results have typical confidence levels of 50% or greater. In many cases we find adequate agreement for a cone size of 1.0 using statistical errors only. This poor agreement for a cone size of 0.7 probably represents the effect of gluon radiation outside the cone, and points to the need for comparison of this quantity with next-to-leading computations which should soon be available.

The CDF central calorimeter can also be used to identify direct photons produced by hard QCD processes. Each projective tower is divided into an interior electromagnetic section (CEM) with 18 radiation lengths of lead absorber, and an exterior hadronic section with iron absorber. A position-sensitive multiwire proportional chamber (CES) is imbedded in the CEM at a depth of 6 radiation lengths. This system is described in detail in [10].

We identify candidate photons as one or two towers of energy in the CEM, with less than 11% hadronic energy and no charged track pointing to the cluster. Jet background can be reduced by requiring the cluster to be isolated, i.e. no more than 15% of the cluster energy is allowed in a cone of $R = 0.7$ around the cluster centroid.

The remaining sample has significant backgrounds dominated by electromagnetic decays of isolated π^0 and η mesons. We subtract this background using two methods. The *profile method* relies on the transverse shower shape of the cluster, as measured in the CES. A χ^2 test is performed to compare the shape of the cluster to that for a standard testbeam electron. On average the χ^2 for photons is smaller than for the

background. We require $\chi^2 < 4$ and evaluate the remaining fraction of background by Monte Carlo simulation. The efficiencies of the cut for background and signal have been checked against electrons from W decay, photons from η decay and π^0s from ρ decay.

The *conversion method* uses the position-sensitive central drift tubes (CDT) to count the number of conversions associated with an electromagnetic cluster. A photon has a conversion probability of approximately 10% in the outer skin material of the CTC, while typical backgrounds have roughly twice this probability. This subtraction technique is independent of photon p_t , which makes it especially useful in the region above 40 GeV, where merging of photons from decays makes the profile method unusable. The two methods give the same cross-section in their common region of p_t .

In figure 4 we show the isolated single photon cross-section from CDF and UA2 [11] compared to next-to-leading order QCD computations [12] (photon bremsstrahlung is only included to leading order). The inner error bars are the statistical error and the outer error bars are the statistical error combined in quadrature with the p_t -dependent part of the systematic error. We show the p_t -independent normalization uncertainty separately. The prediction varies by 30% among common choices of structure functions, and by about 10% when the renormalization scale is halved or doubled. Calculations including bremsstrahlung at next-to-leading order may improve the agreement with the measured results.

This work would have been impossible without the dedication and skill of the Fermilab Accelerator Division, whose assistance we gratefully acknowledge. The work was supported by the U.S. Department of Energy, the National Science Foundation, Instituto Nazionale di Fisica Nucleare, the Ministry of Science, Culture and Education of Japan, and the A.P. Sloan Foundation.

References

[1] F. Paige and S. D. Protopopescu, Brookhaven Report BNL-38034 (1986). G. Marchesini and B.R. Webber, Nucl. Phys. B310,461 (1988). H.U. Bengtsson and G. Ingelman, Computer Phys. Comm. 34,251 (1985).

[2] S. Ellis, Z. Kunst, and D. Soper, Phys. Rev. Lett. 64,2121 (1990).

[3] F. Aversa, M. Greco, P. Chiapetta, and J. Ph. Guillet, LNF-90/012 PT (1990). Submitted to Physical Review Letters.

[4] S. Ellis, "Physics Challenges in the Strong Interactions", in Research Directions for the Decade, Proceedings of the 1990 Summer Study on High Energy Physics, Snowmass, 1990. To be published by World Scientific, 1991.

[5] F. Abe et al. (CDF collaboration), Fermilab Preprint FNAL PUB 91/181 (1991), submitted to Phys. Rev. D.

[6] F. Abe et al. (CDF collaboration), Phys. Rev. Lett. 62,613 (1989).

[7] P. Harriman, A. Martin, R. Roberts, and W. Stirling, Rutherford Laboratory Preprint RAL-90-007 (1990).

[8] J. Morfin and W.K. Tung, Fermilab Preprint FNAL PUB 90/74 (1990).

[9] S. Ellis, private communication.

[10] L. Balka et al., Nucl. Inst. and Meth. A267,272 (1988).

[11] J. Alitti et al. (UA2 Collaboration), CERN Preprint CERN-PPE 91/68, 1991.

[12] P. Aurenche, R. Baier, and M. Fontannaz, Phys. Rev. D42,1440 (1990).

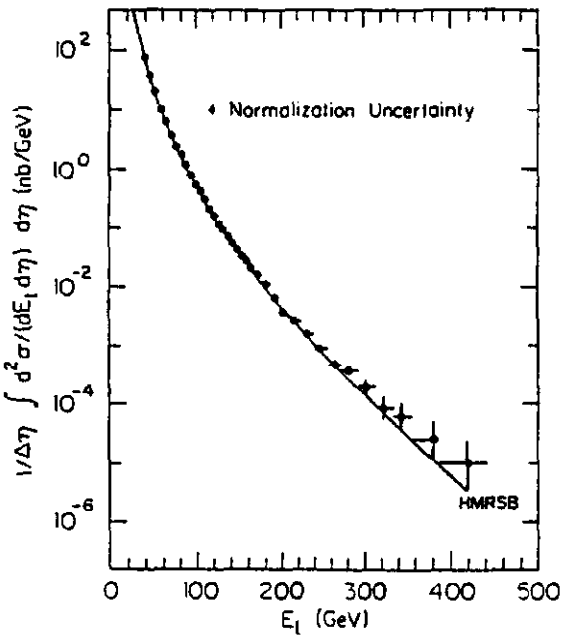

Fig. 1: Inclusive jet E_t spectrum for cone size $R = 0.7$, averaged over $0.1 < |\eta| < 0.7$, compared to theoretical calculation of [2].

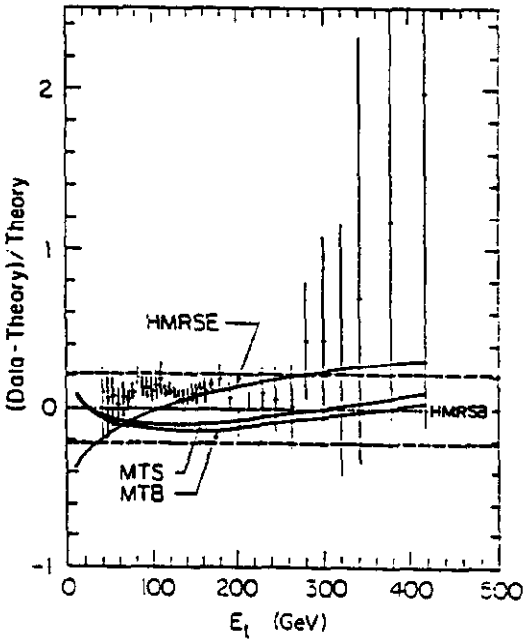

Fig. 2: Jet Inclusive E_t spectrum compared to theory as the ratio of (data-theory)/theory. Dashed lines indicate E_t -independent normalization uncertainty.

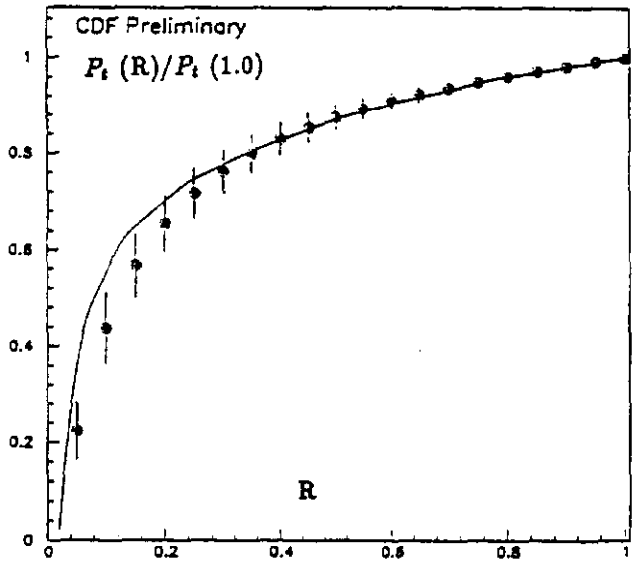

Fig. 3: Integrated p_t distribution within a jet cone of $R = 1.0$ (points), compared with QCD prediction of [9] with $\mu = E_t$ (solid curve). Systematic errors included.

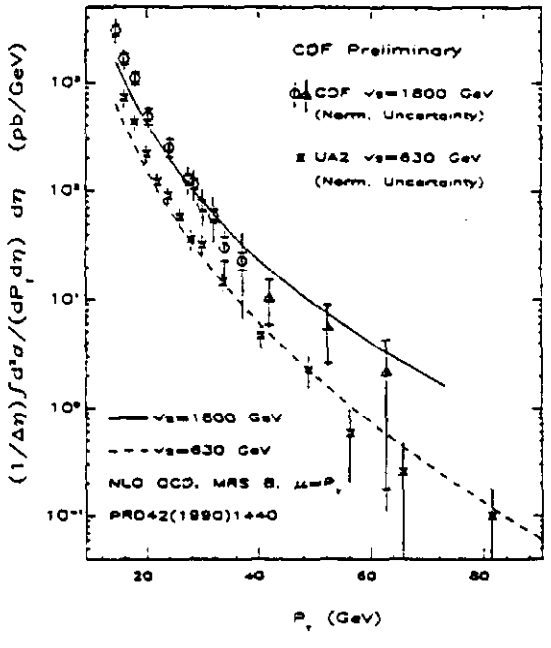

Fig. 4: Isolated prompt photon cross-section compared to QCD prediction of [12].